

A novel multistage system for the detection and removal of pectoral muscles in mammograms

İdil IŞIKLI ESENER^{1,*}, Semih ERGİN², Tolga YÜKSEL¹

¹Department of Electrical & Electronics Engineering, Faculty of Engineering, Bilecik Şeyh Edebali University, Bilecik, Turkey

²Department of Electrical & Electronics Engineering, Faculty of Engineering and Architecture, Eskişehir Osmangazi University, Eskişehir, Turkey

Received: 22.03.2017

Accepted/Published Online: 14.11.2017

Final Version: 26.01.2018

Abstract: In this paper, a novel multistage scheme for pectoral muscle removal from mammography images is proposed, and the performance of this system is verified using the publicly available Mammographic Image Analysis Society digital mammogram database. This database is composed of mediolateral oblique mammography images including three different tissue types (fatty, fatty-glandular, and dense-glandular) with three health status types (normal, benign cancer, and malignant cancer). In the implementation of the proposed system, a mammography image is first preprocessed by performing noise reduction background removal followed by artifact suppression processes. Then a presegmentation procedure is applied using region growing and line fitting is executed. Finally, pixels including pectoral muscle regions are removed from mammography images with an accuracy of 94.40%, sensitivity of 89.62%, and specificity of 99.99% after some postprocessing operations. Although the mean false positive rate obtained by the proposed approach is higher than that of other studies in the literature, not only the lower mean false negative rate but also the enhancement in the quality of pectoral muscle segmentation for all 322 images in the database evidently show the success of the proposed approach.

Key words: Breast cancer, pectoral muscle removal, computer aided diagnosis, digital mammography

1. Introduction

Computer-aided diagnosis (CAD) systems for mammography technology act as a second set of eyes to radiologists for breast cancer detection. The sensitivity of a CAD system is directly affected by suspicious region detection (SRD). In mediolateral oblique (MLO) view mammography images, the presence of pectoral muscles generates an obstacle for SRD since abnormal tissues have intensity characteristics similar to those of pectoral muscles. Hence, a pectoral muscle removal process is surely essential for any CAD systems prior to SRD.

In this paper, a novel multistage scheme for pectoral muscle removal from mammography images is proposed. The publicly available Mammographic Image Analysis Society (MIAS) digital mammogram database is used to verify the performance of the proposed method. Noise reduction, background removal, and artifact suppression are implemented, consecutively, in preprocessing. This stage is followed by the presegmentation stage, where an algorithm for the region growing method (RGM) is proposed and line fitting is executed. Some postprocessing operations are introduced and applied as a subsequent stage to reduce the false positives of

*Correspondence: idil.isikli@bilecik.edu.tr

the results. Finally, the segmented pectoral muscles are removed and mammography images without pectoral muscles are obtained in the last stage.

This paper is organized as follows: a literature overview on pectoral muscle detection is given in the following section. In Section 3, the proposed system for pectoral muscle detection and removal is explicated. The details of the database used in this study and the performance metric employed for the performance evaluation is explained in Section 4. In Section 5, the obtained results, some elaborative comparisons with similar studies in the literature, and detailed discussions are given. The main conclusions are presented in the last section.

2. Related work

Studies on pectoral muscle removal process in the literature generally focus on two different aspects: intensity-based and wavelet-based approaches. These approaches are categorized under three main titles: line detection methods, statistical methods, and other methods [1]. Intensity-based approaches are based on the fact that the intensity range of a pectoral muscle region should be higher than the range of breast parenchyma. These approaches directly utilize the pixel intensities [2–7], image histograms [8–10], and image gradients [11], or they are applied to image gradients [12]. Additionally, there are also some studies that segment pectoral muscles in wavelet domain instead of spatial domain [13–15]. Line-detection methods are also frequently used for pectoral muscle removal in the literature. These methods are based on the fact that a pectoral muscle lies on an upper right/left corner of a mammography image and it has a triangular geometry in general. Line-detection methods aim to determine the hypotenuse of this triangle. For this reason, straight line estimation [4,11,16–21], Hough transform [14,22], and curve fitting [23] are used. The hypotenuse of the triangle pectoral muscle shows a curved structure rather than an exact line. Studies that reveal exact lines using dynamic programming also exist in the literature [16–18,22]. A survey of studies utilizing statistical methods exhibits that graph-based approaches have recently been used for pectoral muscle removal [24–26]. Li et al. and Liu et al. modeled a pectoral muscle region as a variable with normal distribution on the basis that a pectoral muscle is more uniform than a breast parenchyma [27,28]. Liu et al. performed pectoral muscle removal by computing the probability of each pixel to be in the high-frequency region [27]. Additionally, Liu et al. stated that the variance of pectoral muscle contours should be high and pectoral muscles were segmented by the variance calculation. In another study, Moayedi et al. used the logarithm of the pixel energies for pectoral muscle removal [28]. Mean shift segmentation [29], connected component labeling [30], RGM [31–34], RGM combined with geometric rules [35], and fuzzy c-means clustering [36] are some examples of other methods used for pectoral muscle removal in the literature.

3. Proposed system

In this study, a multistage scheme for pectoral muscle removal from mammography images is proposed. Pectoral muscles are the triangle-shaped bright regions lying either on the right or the left top corner in the MLO view mammography images, as shown in the sample image given in Figure 1.

Since pectoral muscles are brighter than breast parenchyma, intensity-based detection methods are effectively suitable for pectoral muscle detection. In view of intensity values, the similarities between pectoral muscle regions and the digitization noise and also the artifacts shown in Figure 1 stand out.

Hence, noise reduction, background removal, and artifact suppression processes are performed on the mammography images, consecutively, as a preprocessing step. Then an algorithm for RGM is applied to the preprocessed images for presegmentation of pectoral muscles. Afterwards, some postprocessing operations are

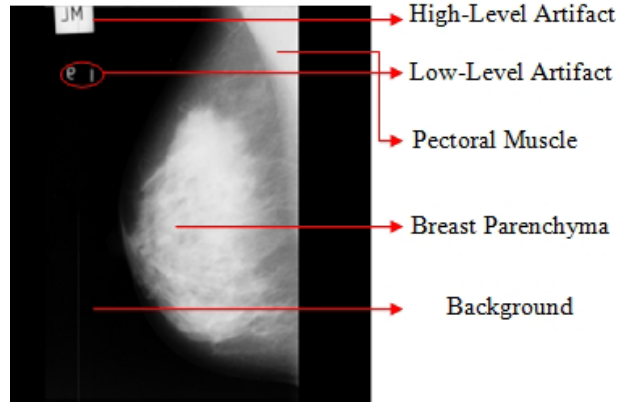


Figure 1. Sample MLO view mammography image.

implemented on the presegmented pectoral muscles in order to reduce the false positives. Finally, the segmented pectoral muscles are removed and the mammography images without pectoral muscles are obtained. A flowchart of the proposed system is shown in Figure 2.

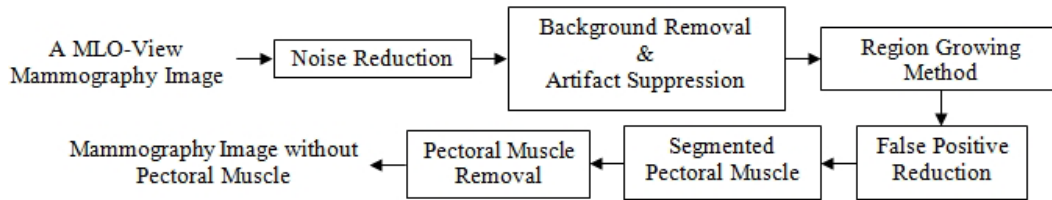


Figure 2. Flowchart of the proposed system.

3.1. Noise reduction

A smoothing filter application is essential for noise reduction, since digitization noise appears as a high-frequency component in images. However, this implementation may result in the loss of significant details. Therefore, adaptive filters are more applicable in order to reduce the noise components while preserving edge details that have essential information in mammography images. The adaptive median filter is a two-level filter that works in an enlargeable rectangular window of size S_{xy} and is capable of removing impulse noise, smoothing other types of noise, and reducing distortion while preserving gross details in an image [37], and it is performed for noise reduction in this study. The pseudocode of the adaptive median filtering is as follows:

Level A : $A1 = z_{med} - z_{min}$

$A2 = z_{med} - z_{max}$

If $A1 > 0$ AND $A2 < 0$, Go to level B

Else increase the window size

f window size $\leq S_{max}$ repeat level A

Else output z_{xy}

Level $B : B1 = z_{xy} - z_{\min}$
 $B2 = z_{xy} - z_{\max}$
 If $B1 > 0$ AND $B2 < 0$, output z_{xy}
 Else output z_{med} ,

where z_{xy} is the gray level at coordinates (x, y) , S_{\max} is the maximum allowed size of S_{xy} , and z_{\min} , z_{\max} , and z_{med} are the minimum gray level, maximum gray level, and median gray levels in S_{xy} , respectively. The initial size of S_{xy} is 3 and S_{\max} is 11 in this study.

3.2. Background removal and artifact suppression

The low- and high-level artifacts shown in Figure 1 are suppressed by applying some morphological operations. In this sense, the mammography images are converted into their binary images by using Otsu's N_o thresholding technique [38] with $N_o = 2$ at first. Then the white areas in each binary image are calculated. Based on the fact that the breast parenchyma should be larger than artifacts, the largest computed area is determined as breast parenchyma. Thus, background removal is also realized by cropping the largest area as well as artifact suppression.

Finally, the pectoral muscle position of each mammography is detected using the method introduced by Nagi et al. [4] so that all images are rearranged. This method initially computes the sum of the first five and last five columns of the background-removed binary image. If the sum of the first five columns is greater than the sum of the last five columns, the method states that the breast profile is right-oriented, or vice versa. By position rearrangement, all pectoral muscles are located in the top left corner of images. The preprocessing stages of a sample mammography image are given in Figure 3.

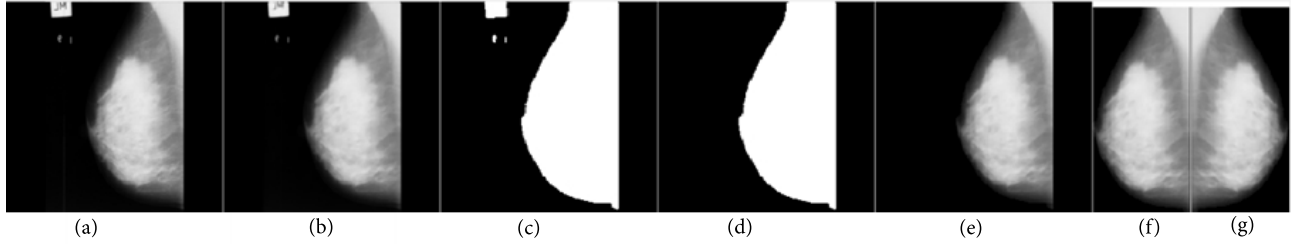


Figure 3. The preprocessing stages of a sample mammography image: (a) Original image, (b) Noise-reduced image, (c) Binary image, (d) Largest area, (e) Breast parenchyma, (f) Background removed image, (g) Preprocessed image.

3.3. RGM

RGM directly segments an image considering a predefined similarity condition [39]. This method is based on enlarging segments by combining pixels with similar properties. For this purpose, first, a seed point or a set of seed points is selected and a similarity metric is defined. Then the selected seed point/set is considered as the startup region and pixels in the 4/8-neighborhood of each pixel in the region are considered in terms of the defined similarity condition. The algorithm continues by combining the similarity condition satisfied neighboring pixels and analyzing the neighborhoods of these pixels until all pixels are examined.

The selection of the initial seed point/set is an important factor affecting the success of the RGM. The initial seed point/set can be selected randomly in the absence of any prior knowledge on the image. In addition,

the selection can be accomplished in accordance with information about the intensity, color, size, and location of a region.

Another issue that affects the success of the method is the definition of similarity condition. The pixel intensities or the spatial features can be used as the similarity condition in gray-level images. The details of the RGM can be found in [39].

The initial step of the proposed pectoral muscle removal process is the presegmentation on the preprocessed mammography images by suggesting an algorithm for the RGM. This algorithm starts with a single seed point and continues by examining the 4-pixel neighborhood in terms of the similarity condition. The similarity condition is defined as the intensity difference between the intensity of pixel that most recently added to the region and the average intensity of the region. As long as this difference is smaller than a predefined maximum difference value, the algorithm continues by combining pixels with the nearest intensity value into the average intensity of the adjoining region P_R . A flowchart of this algorithm is given in Figure 4.

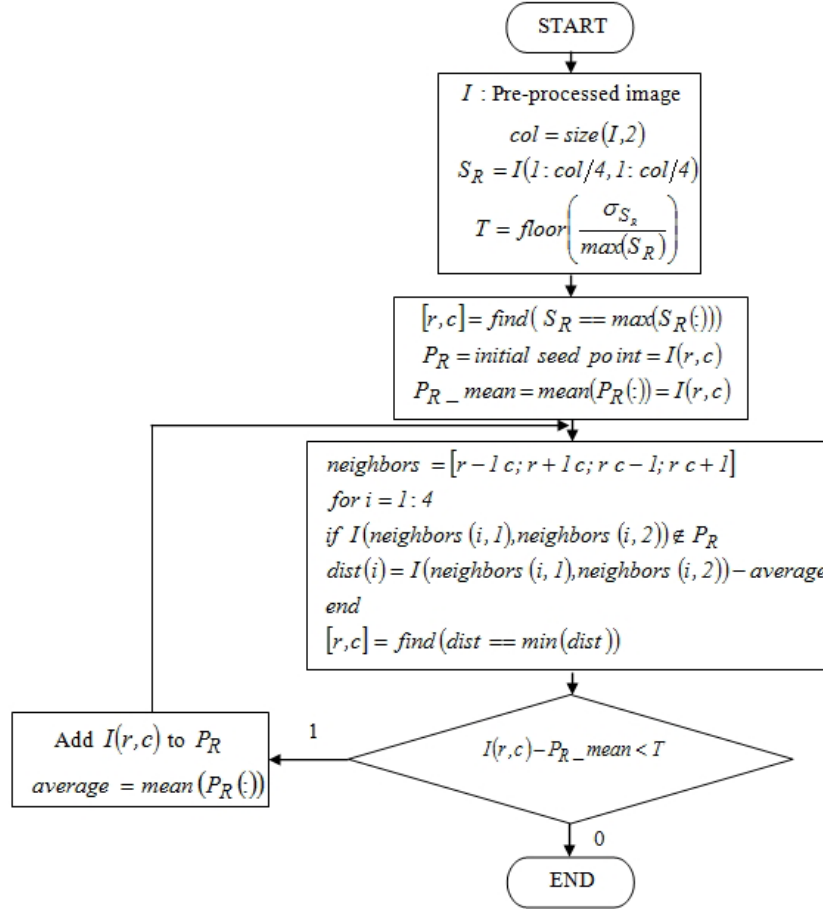


Figure 4. The flowchart of the proposed algorithm for RGM.

The initial seed point is selected considering the facts that a pectoral muscle should lie in the upper left corner in an image and it has a brighter intensity than breast parenchyma. In consequence of these facts, a square region S_R with a column-quarter size on the upper left corner of the preprocessed mammography image is removed automatically for the calculation of the threshold T in the similarity condition $Q(r, c)$; and the

brightest pixel in this region is selected as the initial seed point. This square region of a sample mammography image is shown in Figure 5.

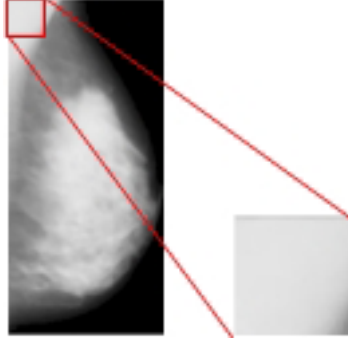


Figure 5. The square region in a sample mammography image.

The threshold (the predefined maximum difference value) in the similarity condition is calculated as the ratio of the standard deviation σ_{S_R} of the region S_R to the maximum value in this region, probable pectoral muscle region, as given in Eq. (1). In this manner, the pixels with intensities much lower than the standard deviation of the probable pectoral muscle region are deliberately excluded.

$$T = \text{floor} \left(\frac{\sigma_{S_R}}{\max(S_R)} \right) \quad (1)$$

The similarity condition $Q(r, c)$ examining for a pixel $I(r, c)$, is formulated as given in Eq. (2). The terms $T, P_R\text{-mean}, r$, and c in the equation indicate the threshold given in Eq. (1), the average intensity of the adjoining region P_R , and row and column coordinates of the pixel in an image I , respectively.

$$Q(r, c) = \begin{cases} 1, & I(r, c) - P_R\text{-mean} < T \\ 0, & \text{otherwise} \end{cases} \quad (2)$$

The goal of applying the RGM using the above mentioned algorithm to mammography images is to segment only pectoral muscles, but whole-breast segmentation has also been encountered in some images. One such image is shown in Figure 6.

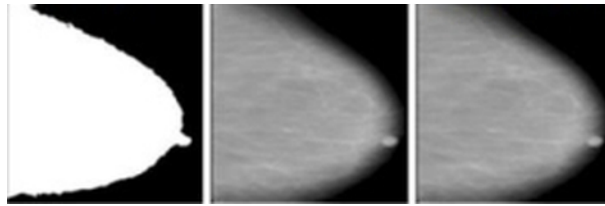


Figure 6. Sample of a whole-breast-segmented mammography image.

These whole-breast-segmented mammography images mostly do not have any pectoral muscle region. Therefore, these images are excluded from the proposed pectoral muscle segmentation procedure. These types of images are determined automatically by checking an area control value of the largest area of the segmented image. Analyzing the images in the MIAS database, it is observed that the pectoral muscle region covers a

maximum of approximately 15% of the breast area. Hence, the area control value is specified as 10,000 pixels for a 256×256 image.

In other cases, for partial-breast-segmented images, the vertices of the triangle shape (points A and B in Figure 7) are determined and a line is fitted to these points. These vertices are determined as the last nonzero pixel of the first nonzero column (point A), and the last nonzero pixel of the first nonzero row (point B) in the image. This scheme is summarized on a sample image in Figure 7.

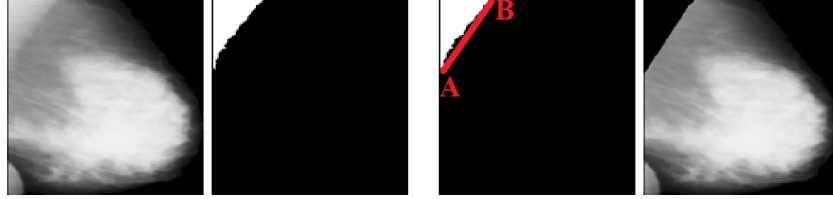


Figure 7. Sample of a pectoral-muscle-segmented mammography image.

In order to reduce the false positive rate in this proposed scheme, two-stage postprocessing operations are examined on the over- or undersegmented pectoral muscles. Determination of presegmented pectoral muscles to be oversegmented or undersegmented is manually realized under an expert radiologist’s consideration. For the first stage, the presegmented pectoral muscles are converted into binary level using a threshold value of T_2 . It is assumed that a presegmented image has no pectoral muscle if the area of the largest area is more than the area control value. Otherwise, the process shown in Figure 7 is applied to the presegmented images.

The threshold value T_2 for the conversion of an image into its binary level image is computed from the region S_{R_2} , which is the upper left square region of the presegmented image with a column-quarter size. This threshold is computed as given in Eq. (3), where N and T are the number of pixels in S_{R_2} and the predefined maximum difference value given in Eq. (1), respectively.

$$T_2 = \begin{cases} \frac{1}{N} \sum_{i=1} S_{R_2}(i), & \frac{1}{N} \sum_{i=1} S_{R_2}(i) \neq 0 \\ T, & \frac{1}{N} \sum_{i=1} S_{R_2}(i) = 0 \end{cases} \quad (3)$$

These images are then binarized assuming self-averages as their threshold values, and the breast contours of the binarized images are detected by using a 7×7 Canny edge detector. Finally, the changes between pectoral muscles and breast parenchyma are identified according to the derivatives of breast contours and the regions under these contours. The proposed pectoral muscle removal approach is shown in Figure 8.

4. Experiments

4.1. Dataset

The MIAS digital mammogram database is used for the verification of the designed multistage scheme for pectoral muscle removal from the mammograms in this study [40]. This database contains left and right whole-breast films of 161 patients in 322 MLO mammography images with three breast tissue types: 106 fatty, 104 fatty-glandular, and 112 dense-glandular tissue types. Some of the images in the database contain more than one abnormality for a total of 330 diagnoses: 207 normal, 69 benign cancers, and 54 malignant cancers. The images are at a resolution of 8 bits/pixel and a size of 1024×1024 in “pgm” imaging format.

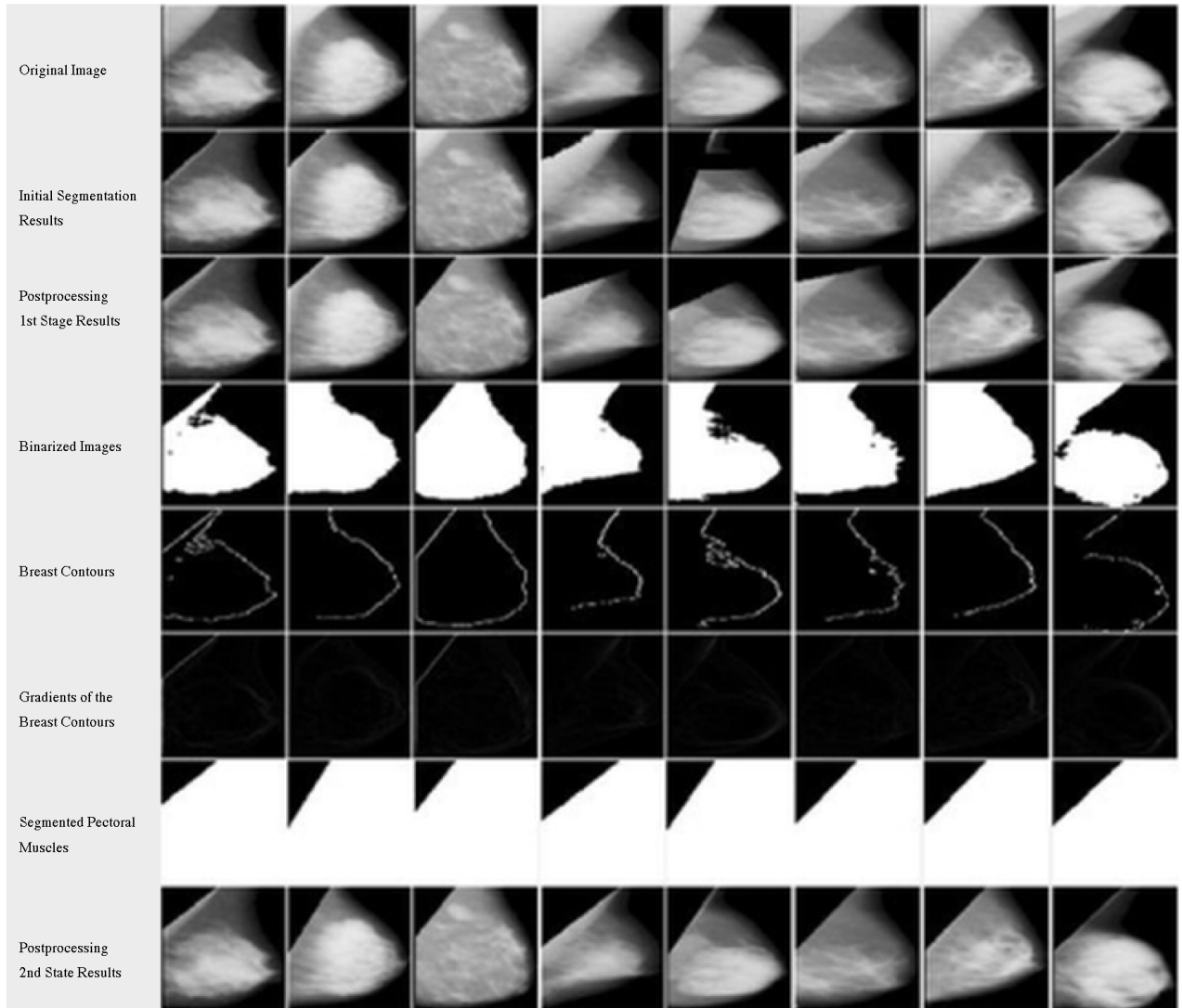


Figure 8. The proposed pectoral muscle removal approach.

All mammography images are resized to a size of 256×256 using bicubic interpolation, for ease of operation. Sample images of each type and diagnosis are shown in Figure 9. The rows and columns in the figure show the diagnoses and the breast tissue types, respectively.

4.2. Performance metrics

In this paper, the area normalized error (ANE) [41] metric is employed for the performance evaluation of the proposed pectoral muscle removal approach, and the achieved results are compared with those of similar studies in the literature. The ground truth of pectoral-muscle-removed mammograms is composed by an expert radiologist manually. The performance metrics (ANE, accuracy, sensitivity, and specificity values) are then calculated by comparing, pixel-wise, the pectoral-muscle-removed image with the ground truth image.

The ANE analyzes the false positive and false negative rates. False positivity in this study is defined as labeling a pixel as being in a pectoral muscle region when it is actually not, as shown in Figure 10.

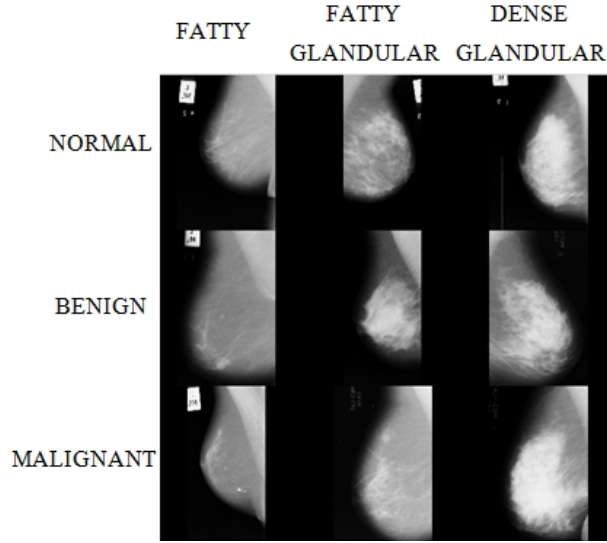


Figure 9. Sample mammography images from the MIAS database.

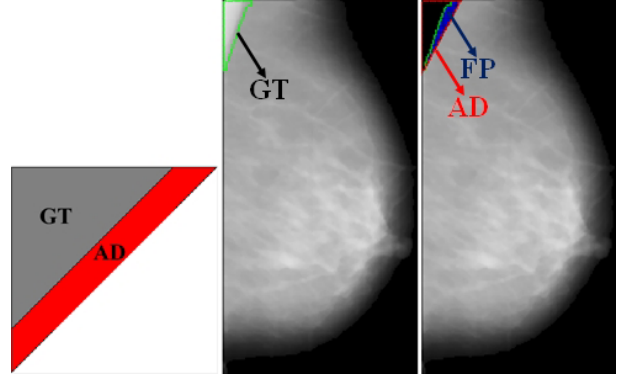


Figure 10. The definition of false positivity.

Conversely, false negativity is when a pixel is actually in a pectoral muscle region, but is detected as a nonpectoral muscle pixel. The definition of false negativity is illustrated in Figure 11.

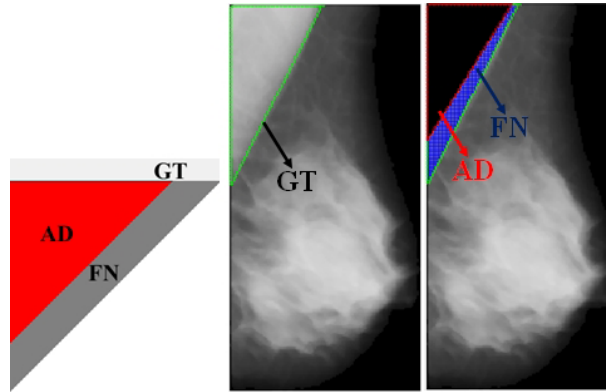


Figure 11. The definition of false negativity.

The regions GT, AD, FP, and FN in the figures show the ground truth of a pectoral muscle, algorithm-defined pectoral muscle, false positives, and false negatives, respectively.

The mathematical representations of mean FP and mean FN rates are given in Eqs. (4) and (5), respectively.

$$FP_m = \frac{1}{A} \sum_{i=1}^p \max[0, B_{alg}(i) - B_{gro}(i)] \quad (4)$$

$$FN_m = \frac{1}{A} \sum_{i=1}^p \max[0, B_{gro}(i) - B_{alg}(i)] \quad (5)$$

The terms A , p , $B_{alg}(i)$, and $B_{gro}(i)$ in the equations refer to the area of the reference pectoral muscle, total number of rows in a pectoral muscle region, the boundary pixel in the i th row of the algorithm defined pectoral muscle, and the boundary pixel in the i th row of the reference pectoral muscle, respectively.

The accuracy, sensitivity, and specificity values are calculated as given in Eqs. (6)–(8), respectively.

$$\text{Accuracy} = \frac{TP}{TP + FP + TN + FN} \quad (6)$$

$$\text{Sensitivity} = \frac{TP}{TP + FN} \quad (7)$$

$$\text{Specificity} = \frac{TN}{TN + FP} \quad (8)$$

The terms TP , TN , FP , and FN in the equations refer to the total number of true positive, true negative, false positive, and false negative pixels calculated when the pectoral-muscle-removed images are pixel-wise registered with the ground truth images, respectively.

5. Results

In this section, the results of the proposed system according to performance metrics that are valid in the literature are given. Firstly, the RGM using the proposed algorithm shown in Figure 4 is directly applied to the preprocessed mammography images, and the presegmented pectoral muscles are obtained. Although it is intended to segment only pectoral muscles, whole-breast segmentation has also been encountered in some images. In other cases, for partial-breast-segmented images, the line-fitting operation shown in Figure 7 is performed. Then the area above this line is defined as the pectoral muscle with an accuracy of 52.48% approved by an expert radiologist.

In some cases where the pixel intensities of the pectoral muscle region are quite similar to the pixel intensities of breast parenchyma, as shown in Figure 12, the proposed system is not capable of segmenting pectoral muscles. Hence, it concludes with an incorrect breast segmentation. In order to overcome this problem, the system equalizes the histogram of images before applying the above process. The success rate for the segmentations of pectoral muscles is then increased to 63.04%.



Figure 12. Sample of an incorrect breast-segmented mammography image.

In order to reduce the false positive rate in this proposed system, the two-stage post processing operations mentioned before are performed. The success rate is increased to 74.84% by the first stage of postprocessing, and the pectoral muscles of 304 images of the MIAS database over 322 images are removed so that an accuracy rate of 94.40% is accomplished by the second stage postprocessing. Furthermore, sensitivity and specificity rates are obtained as 89.62% and 99.99% for the proposed system, respectively.

The attained results calculated by the ANE metric and the comparison of the proposed study with other studies in the literature are given in the Table. The mean FP rate obtained by the proposed approach is higher than that of other studies. This outcome indicates that our algorithm defines more pixels as being in a pectoral muscle region while they are actually not. In contrast, the lowest FN_m rate is achieved using our proposed approach. In addition, the approach gains higher-quality results, including smaller errors, in all 322 mammography images, since both the FP_m and FN_m terms are less than 0.05. The highest rate for this criterion is obtained using the method of Eigenvectors segmentation, which is about 64% among other studies in the Table. The increment in higher quality results and the decrement in the FN_m rate clearly verify the success of the proposed approach.

6. Conclusion

This study focuses on pectoral muscle removal from MLO-view mammography images. A multistage system for this goal is proposed and it is elaborately verified using the MIAS digital mammogram database. The proposed approach is designed pursuant to the positional and geometrical information of pectoral muscles. Initially, mammography images are preprocessed performing noise reduction followed by background removal and artifact suppression processes. Then an algorithm for the RGM is proposed and applied to preprocessed mammography images. This method is based on positional information of muscles, and then it is followed by a line fitting in compliance with some geometrical characteristics of muscles. The results show that this process is incapable when pixel intensities of a pectoral muscle and a breast parenchyma are quite similar. In order to overcome this problem, the system firstly equalizes histograms of preprocessed images, and then the region growing process is performed. Finally, some postprocessing operations are employed for reducing the number of false positives, and consequently a segmentation accuracy of 94.40%, sensitivity of 89.62%, and specificity of 99.99% are obtained.

The ANE is used as a metric in order to evaluate the performance of the proposed system. When one compares the proposed system with the other approaches in the literature, the average rate obtained for false positives is higher than those in the other studies. The reason for this result is that more than enough pixels are determined as a pectoral muscle region. In addition, the lower-most average rate is attained for false negatives using our proposed system among all studies. Since not only the false positive but also the false negative metrics give less than 0.05, our multistage system generates higher-quality results, including smaller errors, compared to the other approaches for all 322 mammography images. In the comparative studies, the maximum rate for this criterion is about 64% and it is obtained by utilizing Eigenvectors segmentation [26]. Therefore, one can easily infer that the reduction in the average rate for false negatives and the enhancement in the quality of pectoral muscle segmentation obviously prove the success of the proposed approach.

In this study, a novel system with noise reduction based on adaptive median filter, background removal, and artifact suppression depending on Otsu's thresholding method and Nagi's breast orientation method and segmentation based on a modified RGM algorithm is proposed for pectoral muscle removal. The results of performance metrics prove that the proposed system is superior to other approaches. From the theoretical point of view, the authors think that the proposed system has a quite simpler structure than the methods in the Table according to computational complexity. In addition to the success of the proposed approach, the computational time of this approach is under 1 s, which is also suitable to be implemented in a real-time CAD system. It is clear that wavelet- and transformation-based methods reveal computational burdens that may cause delayed CAD results.

While RGM is a common approach for image segmentation, using this method directly for mammography

Table. The comparison of the results using the evaluation of the eight different criteria for pectoral muscle removal.

Evaluation criterion	Proposed	Eigenvectors	Hough	Gabor	Adaptive	Minimum	Graph-cut based	Watershed
	approach	segmentation	transform	wavelets	pyramid	spanning tree	merging	transformation
FP_m (mean false positivity)	0.0415	0.0074	0.0198	0.0058	0.0371	0.0255	0.0064	0.0085
FN_m (mean false negativity)	0.0328	0.0412	0.2519	0.0577	0.0595	0.1168	0.0558	0.0488
$FP < 0.05$ & $FN < 0.05$	322	51	10	45	50	40	43	46
$\min(FP, FN) < 0.05$ & $0.05 < \max(FP, FN) < 0.10$	0	18	0	0	18	20	19	25
$\min(FP, FN) < 0.05$ & $\max(FP, FN) > 0.10$	0	10	0	0	11	18	22	13
$0.05 < FP < 0.10$ & $0.05 < FN < 0.10$	0	1	8	22	0	0	0	0
$0.05 < \min(FP, FN) < 0.10$ & $\max(FP, FN) > 0.10$	0	—	0	0	0	1	0	0
$FP > 0.10$ & $FN > 0.10$	0	0	66	17	5	3	0	0

images with whole breasts without pectoral muscles causes false results, and a simple algorithm is proposed in the study to exclude these images from evaluation. This approach clearly shows that segmentation approaches should be modified to overcome this problem.

The study also proposes practical and reliable solutions to increase the performance of the proposed system. Therefore, the study highlights the problems of pectoral muscle removal and it provides a basis for pectoral removal studies.

It is planned to integrate this system into a CAD system that includes classification of tissue and health types of mammogram images for future studies. It is clear that the performance of the proposed system will affect the performance of the CAD system.

References

- [1] Ganesan K, Acharya UR, Chua KC, Min LC, Abraham KT. Pectoral muscle segmentation: A review. *Comput Meth Prog Bio* 2013; 110: 48-57.
- [2] Saltanat M, Hossain MA, Alam MS. An efficient pixel value based mapping scheme to delineate pectoral muscle from mammograms. In: *IEEE 2010 International Conference on Bio-Inspired Computing: Theories and Applications*; 23–26 September 2010; Changsha, China. New York, NY, USA: IEEE. pp. 1510-1517.
- [3] Roshan DY, Harada K. A connected component labelling algorithm for grayscale images and application of the Algorithm on mammograms. In: *2007 Annual ACM Symposium on Applied Computing*; 11–15 March 2007; Seoul, Republic of Korea. New York, NY, USA: ACM. pp. 146-152.
- [4] Nagi J, Kareem SA, Nagi F, Ahmed SK. Automated breast profile segmentation for ROI detection using digital mammograms. In: *IEEE 2010 EMBS Conference on Biomedical Engineering & Sciences*; 30 November–2 December 2010; Kuala Lumpur, Malaysia. New York, NY, USA: IEEE. pp. 87-92.
- [5] Liu L, Wang J, He K. Breast density classification using histogram moments of multiple resolution histograms. In: *2010 International Conference on Biomedical Engineering and Informatics*; 16–18 October 2010; Yantai, China. New York, NY, USA: IEEE. pp. 146-149.
- [6] Liu CC, Tsai CY, Liu J, Yu CY, Yu SS. A pectoral muscle segmentation algorithm for digital mammograms using Otsu thresholding and multiple regression analysis. *Comput Math Appl* 2012; 64: 1100-1107.
- [7] Kurt B, Nabiyeve VV, Turhan K. A novel automatic suspicious mass regions identification using Havrda & Charvat entropy and Otsu's N thresholding. *Comput Meth Prog Bio* 2014; 114: 349-360.
- [8] Thangavel K, Karnan M. Computer aided diagnosis in digital mammograms: Detection of microcalcifications by meta heuristic algorithms. *Int J Artif Intell Mach Learn* 2005; 5: 29-40.
- [9] David R, Arnau O, Joan M, Marta P, Joan E. Breast segmentation with pectoral muscle suppression on digital mammograms. *Lect Notes Comput Sc* 2005; 153-158.
- [10] Subashini T S, Ramalingam V, Palanivel S. Pectoral muscle removal and detection of masses in digital mammogram using CCL. *Int J Comput Appl* 2010; 1: 71-76.
- [11] Chakraborty J, Mukhopadhyay S. Automatic detection of pectoral muscle using average gradient and shape based feature. *J Digit Imaging* 2012; 25: 387-399.
- [12] Camilus KS, Govindan VK, Sathidevi PS. Pectoral muscle identification in mammograms. *J Appl Clin Med Phys* 2011; 12: 215-230.
- [13] Mustra M, Bozek J, Grgic M. Breast border extraction and pectoral muscle detection using wavelet decomposition. In: *IEEE 2009 International Conference on Computer as a Tool*; 18–23 May 2009; St. Petersburg, Russia. New York, NY, USA: IEEE. pp. 1426-1433.
- [14] Ferrari RJ, Rangayyan RM, Desautels JEL, Borges RA, Frere AF. Automatic identification of the pectoral muscle in mammograms. *IEEE T Med Imaging* 2004; 23: 232-245.

- [15] Ma WY, Manjunath BS. Edge flow: A technique for boundary detection and image segmentation. *IEEE T Image Process* 2000; 9: 1375-1388.
- [16] Karssemeijer N. Automated classification of parenchymal patterns in mammograms. *Phys Med Biol* 1998; 43: 365-378.
- [17] Kwok SM, Chandrasekhar R, Attikiouzel Y. Automatic pectoral muscle segmentation on mammograms by straight line estimation and cliff detection. In: *IEEE 2001 Australian and New Zealand Intelligent Information Systems Conference*; 18–21 November 2001; Perth, Western Australia. New York, NY, USA: IEEE. pp. 67-72.
- [18] Kwok SM, Chandrasekhar R, Attikiouzel Y, Rickard MT. Automatic pectoral muscle segmentation on mediolateral oblique view mammograms. *IEEE T Med Imaging* 2004; 23: 1129-1140.
- [19] Mustra M, Grgic M. Robust automatic breast and pectoral muscle segmentation from scanned mammograms. *Signal Process* 2013; 93: 2817-2827.
- [20] Tzikopoulos SD, Mavroforakis ME, Georgiou HV, Dimitropoulos N, Theodoridis S. A fully automated scheme for mammographic segmentation and classification based on breast density and asymmetry. *Comput Meth Prog Bio* 2011; 102: 47-63.
- [21] Vaidehi K, Subashini TS. Automatic identification and elimination of pectoral muscle in digital mammograms. *Int J Comput Appl* 2013; 75: 15-18.
- [22] Yam M, Brady M, Highnam R, Behrenbruch C, English R, Kita Y. Three-dimensional reconstruction of microcalcification clusters from two mammographic views. *IEEE T Med Imaging* 2001; 20: 479-489.
- [23] Weidong X, Lihua L, Wei LA. Novel pectoral muscle segmentation algorithm based on polyline fitting and elastic thread approaching. In: *2007 International Conference on Bioinformatics and Biomedical Engineering*; 6–8 July 2007; Wuhan, China. New York, NY, USA: IEEE. pp. 837-840.
- [24] Domingues I, Cardoso JS, Amaral I, Moreira I, Passarinho P, Comba JS, Correia R, Cardoso MJ. Pectoral muscle detection in mammograms based on the shortest path with endpoints learnt by SVMs. *Eng Med Biol* 2010; 3158-3161.
- [25] Camilus KS, Govindan VK, Sathidevi PS. Computer-aided identification of the pectoral muscle in digitized mammograms. *J Digit Imaging* 2010; 23: 562-580.
- [26] Abdellatif H, Taha TE, Zahran OF, Al-Nauimy W, El-Samie FEA. Automatic pectoral muscle boundary detection in mammograms using eigenvectors segmentation. In: *2012 International Radio Science Conference*; 10–12 April 2012; Cairo, Egypt. New York, NY, USA: IEEE. pp. 633-640.
- [27] Liu L, Wang J, Wang T. Breast and pectoral muscle contours detection based on goodness of fit measure. In: *2011 International Conference on Bioinformatics and Biomedical Engineering*; 10–12 May 2011; Wuhan, China. New York, NY, USA: IEEE. pp. 1-4.
- [28] Moayed F, Azimifar Z, Boostani R, Katebi S. Contourlet-based mammography mass classification using the SVM family. *Comput Biol Med* 2010; 40: 373-383.
- [29] Sultana A, Ciuc M, Strungaru R. Detection of pectoral muscle in mammograms using mean-shift segmentation approach. In: *IEEE 2010 International Conference on Communications*; 23–27 May 2010; Cape Town, South Africa. New York, NY, USA: IEEE. pp. 165-168.
- [30] Li JB. Mammographic image based breast tissue classification with kernel self-optimized fisher discriminant for breast cancer diagnosis. *J Med Syst* 2012; 36: 2235-2244.
- [31] Maitra IK, Nag S, Bandyopadhyay SK. Technique for preprocessing digital mammogram. *Comput Meth Prog Bio* 2012; 107: 175-188.
- [32] Talha M, Sulong GB. Preprocessing and pectoral muscle separation from breast mammograms. *Int J Phys Sci* 2012; 7: 471-477.
- [33] Anitha J, Peter JD, Pandian SIA. A dual stage adaptive thresholding (DuSAT) for automatic mass detection in mammograms. *Comput Meth Prog Bio* 2017; 138: 93-104.

- [34] Guo Y, Dong M, Yang Z, Gao X, Wang K, Luo C, Ma Y, Zhang J. A new method of detecting micro-calcification clusters in mammograms using contourlet transform and non-linking simplified PCNN. *Comput Meth Prog Bio* 2016; 130: 31-45.
- [35] Taghanaki SA, Liu Y, Miles B, Hamarneh G. Geometry based pectoral muscle segmentation from MLO mammogram views. *IEEE T Bio-Med Eng* 2017; in press.
- [36] Feudjio CK, Klein J, Tiedeu A, Colt O. Automatic extraction of pectoral muscle in the MLO view of mammograms. *Phys Med Biol* 2013; 58: 8493.
- [37] Gonzalez RC, Woods RE. Image restoration. In: *Digital Image Processing*. 2nd ed. Upper Saddle River, NJ, USA: Prentice Hall, 2004, pp. 241-243.
- [38] Otsu N. A threshold selection method from gray-level histograms. *IEEE T Syst Man Cyb* 1979; 9: 62-66.
- [39] Gonzalez RC, Woods RE. Image segmentation. In: *Digital Image Processing*. 3rd ed. Upper Saddle River, NJ, USA: Prentice Hall, 2008. pp. 711-816.
- [40] Suckling J, Parker J, Dance DR, Astley S, Hutt I, Boggis CRM, Ricketts I, Stamatakis E, Cerneaz N, Kok SL et al. The mammographic image analysis society digital mammogram database. *Exerpta Medica* 1994; International Congress Series 1069: 375-378.
- [41] Ma F, Bajger M, Slavotinek JP, Bottema MJ. Two graph theory based methods for identifying the pectoral muscle in mammograms. *Pattern Recogn* 2007; 40: 2592-2602.